

# Giant optical nonlinearity of plasmonic nanostructures

P.N. Melentiev, A.E. Afanasiev, V.I. Balykin

**Abstract.** The experimental studies of giant optical nonlinearity of single metal nanostructures are briefly reviewed. A new hybrid nanostructure – split-hole resonator (SHR) – is investigated. This structure is characterised by a record-high efficiency of third-harmonic generation and multiphoton luminescence (its nonlinearity exceeds that of a single nanohole by five orders of magnitude) and an unprecedentedly high sensitivity to light polarisation (extinction coefficient  $4 \times 10^4$ ).

**Keywords:** nanoplasmonics, nonlinear optics, third-harmonic generation, nanolocalised light source.

## 1. Introduction

An important property of metal nanostructures is their strong optical nonlinearity, which is caused by collective motion of free electrons in metal. For example, the third-order nonlinear susceptibility of gold is three orders of magnitude higher than that of nonlinear KDP, KTP, or LiNbO<sub>3</sub> crystals [1]. To date, nonlinear nanoplasmonics studies the following processes in nanostructures: second-harmonic generation [2–7]; four-wave mixing [8]; high-harmonic generation [9, 10]; ultrafast optical modulation, which is based on third-order optical nonlinearity [11–14]; and multiphoton luminescence [15–19].

In this work, we proposed and investigated a new element of nanoplasmonics with unique properties: a hybrid nanostructure of split-hole resonator (SHR) type, which makes it possible to implement an unprecedentedly high efficiency of nonlinear processes of third-harmonic generation (THG) and multiphoton luminescence (on the order of unity for a single nanostructure) and record-high sensitivity to light polarisation (extinction coefficient  $\sim 4 \times 10^4$ ). The presence of strong plasmon resonance in an SHR nanostructure (SHR NS) makes it possible to develop an efficient nanolocalised THG source. We demonstrated an all-optical control of light emission from these SHR NS's with a spatial resolution of about  $\lambda/3$ , without sharp beam focusing.

## 2. SHR as an efficient element of nanoplasmonics

Figure 1 illustrates the basic concept of design and functioning of an SHR NS [20], which consists of a nanorod (Fig. 1a)

and a nanohole (Fig. 1b), formed in a metal nanofilm. The lower part of Fig. 1 shows the calculated distributions of electric field intensity in these nanostructures irradiated by a plane monochromatic wave at  $\lambda = 1.5 \mu\text{m}$ , which corresponds to the plasmon resonance in an SHR NS, and its components (nanorod and nanohole) (Fig. 1c).

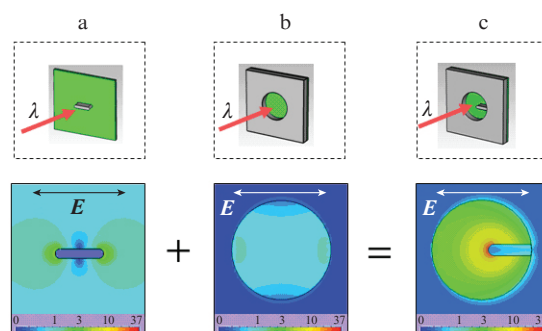


**Figure 1.** Principle of designing an SHR nanostructure and its operation [20]. An SHR structure (c) consists of a nanorod (a) and a nanohole (b) formed in a metal nanofilm. Calculated (by the FDTD method) spatial distributions of near-field intensity are shown in the bottom for a  $(50 \times 180)$ -nm aluminium nanorod, a 380-nm nanohole in a 100-nm-thick aluminium film, and SHR NS, respectively. The incident light wavelength is  $\lambda = 1560$  nm.

The calculated spatial distributions of the electric-field amplitude show some characteristic features of SHR NS's. As can be seen in Fig. 1, the SHR forms a single-pole antenna with a field localised near the nanorod tip. In addition, the maximum field amplitude in SHR NS's is an order of magnitude larger than the maximum field for a single nanorod. The reason is that the nanorod length is much smaller than the resonant length for the chosen frequency of incident wave, and plasmon resonance in a nanorod is implemented only when its length is approximately equal to half plasmon wavelength. Thus, the SHR NS geometry allows one to implement plasmon resonance at smaller linear geometric sizes of nanostructure.

A comparison of SHR NS's with other known single-pole nanoantennas (dual nanodisks, butterfly-type nanoantennas, etc.) shows that, all other factors being equal, it has (being considered as a nanoantenna) smaller geometric sizes for implementing plasmon resonance; this is important from the practical point of view.

SHR NS's, along with other nanostructures, can be considered as a nanolocalised light source, which has a number of advantages. First, it is the absence of related background of excitation light (which is always present in the case of nanoparticles and is generally very high). Second, the trans-

P.N. Melentiev, A.E. Afanasiev, V.I. Balykin Institute of Spectroscopy, Russian Academy of Sciences, ul. Fizicheskaya 5, Troitsk, 142190 Moscow, Russia; e-mail: balykin@isan.troitsk.ru

Received 3 March 2014; revision received 14 March 2014  
Kvantovaya Elektronika 44 (6) 547–551 (2014)  
Translated by Yu.P. Sin'kov

mittance of light through SHR NS's is much higher than through a nanohole of the same size. In addition, since a SHR is formed in a metal film, it may withstand incident light of higher intensity in comparison with isolated nanoparticles and, correspondingly, is a more efficient nonlinear element for laser light conversion.

### 3. Formation of an SHR and its optical and spectral characteristics

We used aluminium as a material for SHR. Investigations were performed at a wavelength  $\lambda = 1560$  nm, in the vicinity of which aluminium exhibits strong nonlinear optical properties: the optical nonlinearity  $\chi^{(3)}$  of aluminium exceeds that of gold by a factor of about 1000 [21, 22]. In addition, radiation with a wavelength  $\lambda = 1560$  nm is widely used in modern telecommunication systems. SHR nanostructures in the geometry presented in Fig. 1b were formed by a focused ion beam in a 100-nm-thick aluminium film.

When studying the optical and spectral properties of SHR NS's, we irradiated them with a pulsed laser beam ( $\tau = 120$  fs, power 15 mW) focused into a spot 4.5  $\mu\text{m}$  in diameter. All measurements were performed with single SHR's. Two nonlinear optical processes were investigated: THG and multiphoton photoluminescence. The details of sample preparation and the technique for detecting and processing signals were reported in [20–23].

#### 3.1. Third-harmonic generation

Figure 2 shows the results of measuring THG from a single SHR NS with a hole diameter of 380 nm. The calculated spatial distribution of the electric field intensity in a nanostructure irradiated by a plane monochromatic wave is shown in Fig. 2b. One can see that this distribution at the fundamental frequency has a pronounced maximum and is localised in the SHR NS (near the nanorod tip). In turn, this field is a source of induced third-order polarisation, which leads to THG. As can be seen in Fig. 2b, spatial localisation of the third-harmonic source is determined by the transverse nanorod size, which is about 120 nm. The optical image of the nanostructure (obtained with a Nikon Ti inverted microscope at a wavelength of 520 nm) contains a diffraction-limited spot with an FWHM of about 230 nm (Fig. 2c). The elliptical shape of this spot indicates that the recorded radiation is polarised in the direction orthogonal to

the polarisation direction of excitation light. The SHR NS emission spectrum consists of a narrow line at the THG frequency of the excitation wave (Fig. 2d).

Our calculations and measurements showed that the THG efficiency of SHR NS's depends strongly on its geometry (nanostructure diameter, nanorod length, and film thickness), film material, and the refractive index of the SHR medium [20, 23]. This behaviour is explained by the known strong dependence of the efficiency of excitation localised plasmon oscillations on the geometry of the nanostructure and its local environment, which determine the distribution and amplitude of the electromagnetic field near the nanostructure. We should note that the dependence of THG efficiency on the SHR hole diameter and the SHR nanorod length has a strong resonant character. The resonant behaviour of SHR NS's, revealed in our calculations, can be interpreted as follows. A plasmon wave propagates through a nanostructure along the metal–insulator interface, formed by the SHR hole perimeter. The nanorod acts as a set of mirrors, from which the plasmon wave is reflected. If the length of the perimeter of the hole forming the nanostructure contains an integer number of plasmon half-wavelengths, resonances of Fabry–Perot type are excited in the nanostructure. The nanorod length determines the plasmon wave reflectance and phase shift.

We performed THG measurements for two nanostructures: (i) structure with 200-nm nanoholes and (ii) an SHR NS [20]. They both have the same open-surface area; however, as measurements showed, the conversion efficiency to the third harmonic for the SHR NS exceeds that for the nanohole by almost five orders of magnitude. The absolute value of the conversion efficiency into the third harmonic (the ratio of the third-harmonic intensity to the fundamental-wave intensity) per unit area is  $10^{-5}$ ; this is a record-high value for the experiments on THG in single nanostructures.

Note that an increase in the excitation intensity by a factor of 50 (to  $5 \times 10^{11}$  W  $\text{cm}^{-2}$ ) should increase the THG efficiency to a value close to unity. As calculations show, irradiation with this intensity does not cause thermal destruction of the nanostructure. The maximum temperature on the SHR NS surface does not exceed 300 K, which is much below the melting temperature of the nanostructure. Note also that the radiation intensity is below the metal fracture threshold, because intense femtosecond radiation induces plasma formation. Thus, an SHR NS is a promising candidate for a nanolocalised third-harmonic source with close-to-unity efficiency.

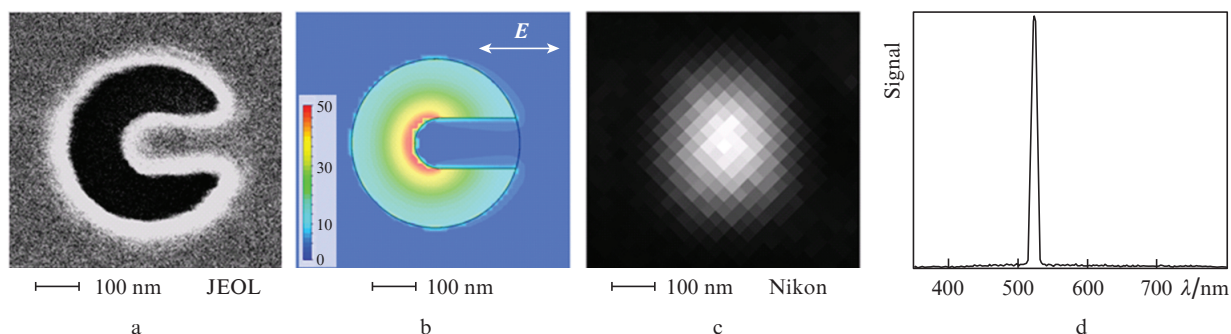


**Figure 2.** Third-harmonic generation from an SHR NS fabricated in a 100-nm-thick aluminium film [20]: (a) electron-microscope image of the nanostructure; (b) a calculated field intensity distribution in the nanostructure exposed to a plane monochromatic wave with  $\lambda = 1560$  nm; (c) an optical image of the nanostructure exposed to light with  $\lambda = 1560$  nm, recorded at the THG wavelength (520 nm); and (d) measured THG spectrum. The light polarisation vector is directed along the nanorod.

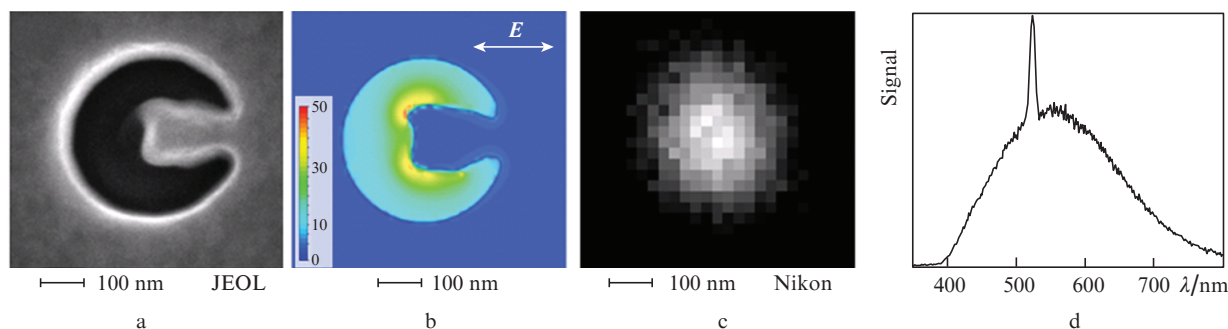


**Figure 3.** Multiphoton luminescence from an SHR NS fabricated in a 100-nm-thick aluminium film [20]: (a) electron-microscope image of the nanostructure; (b) calculated amplification of electric field intensity in an SHR NS exposed to a plane monochromatic wave at  $\lambda = 1560$  nm; (c) optical image of the nanostructure irradiated with a laser beam at  $\lambda = 1560$  nm, recorded in the spectral range of 400–800 nm; and (d) the multiphoton luminescence spectrum.

### 3.2. Multiphoton luminescence

Multiphoton luminescence is due to the excitation of electron surface states localised on the metal surface, which arise on nanosized inhomogeneities of the aluminium film surface [15–19]. To excite multiphoton luminescence in SHR, we formed nanosized inhomogeneities on the nanorod tip, where the field intensity is maximal at the fundamental frequency. Inhomogeneities were formed by an ion beam (FEI Quanta 3D); their sizes ranged from 5 to 15 nm (Fig. 3). The other geometric sizes of SHRs with inhomogeneities were the same as for the smooth SHR NS's presented in Fig. 2. Our calculations showed that the optical linear properties (transmission of light and scattering) of this nanostructure do not differ from the optical properties of a nanostructure with a smooth nanorod.

This SHR NS was exposed to radiation with the same parameters as for the nanostructure in Fig. 2. Figure 3 shows the results of studies on excitation of multiphoton luminescence in a single SHR NS with irregularities. The calculated field distribution of the nanostructure is presented in Fig. 3b. One can see that the spatial distribution of the fundamental-frequency field contains a pronounced maximum near the nanorod tip. The optical image of SHR, obtained with a Nikon Ti/U microscope (objective 40 $\times$ , NA = 0.65) at the luminescence wavelength, is a diffraction-limited spot (Fig. 3b). This spot, in contrast to the optical image in Fig. 2b, has a round shape, because the luminescence light is depolarised. The SHR NS emission spectrum consists of a narrow THG peak and a broadband continuum in the range from 390 to more than 800 nm (Fig. 3d). This broadband continuum is due to the multiphoton luminescence. As measurements showed, its power depends on the excitation intensity  $I$  as  $I^{3.3}$ .

The sizes and shape of the nanostructure in nanoplasmonics determine to a great extent the resonant plasmon frequencies and, as a consequence, its scattering spectrum. To design a nanostructure with specified optical properties, one must control its geometry with an error no larger than  $\sim \lambda/10$ . The demonstrated radical change in the spectrum of nonlinear optical conversion of the SHR NS with a change in its geometry convincingly shows that the nanostructure geometry in nonlinear nanoplasmonics must be controlled with an error smaller than  $\lambda/100$ .

### 3.3. Polarisation effects in the SHR

The SHR NS geometry has a pronounced anisotropy, which is determined by the nanorod direction. In turn, the presence

of anisotropy suggests that the SHR optical response depends on the polarisation of incident light. We investigated the polarisation dependence of the SHR response by an example of THG. The near-field distribution was calculated at the excitation frequency for the cases of incident light polarised perpendicular to the nanorod and along it. A relative change in the field intensity at the fundamental frequency with a change in polarisation does not exceed 40. The experimental dependence of the THG signal from the SHR NS on the excitation light polarisation is shown in Fig. 4. It can be seen that the THG signal is minimal when the light is polarised perpendicular to the nanorod. A rotation of the polarisation vector by 90 $^\circ$  leads to an increase in the THG power by a factor of 40000! This extremely high sensitivity to the polarisation of incident light is due to the cubic dependence of the THG efficiency on the incident intensity.

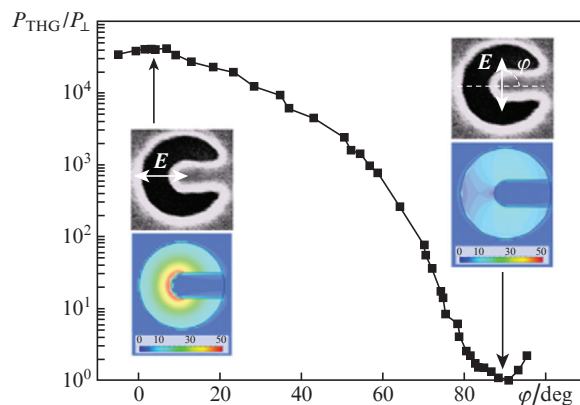


**Figure 4.** Dependence of the THG intensity on the excitation light polarisation for SHR NS's. The insets show the calculated enhancement of electric field intensity for the incident light in the SHR at maximum and minimum THG powers. The maximum relative change in the field intensity near the SHR nanorod under rotation of the plane of polarisation of incident light is about 50.

The strong dependence of the SHR THG efficiency is important for practical applications in optical sensorics and ultrafast optical switches. We demonstrated the use of SHR NS's in designing a prototype of an all-optical display, in which pixels are individual SHR NS's.

This optical display is an array of 4 $\times$ 4 identical SHR NS's with a distance of 1  $\mu$ m between neighbouring SHRs (Fig. 5).

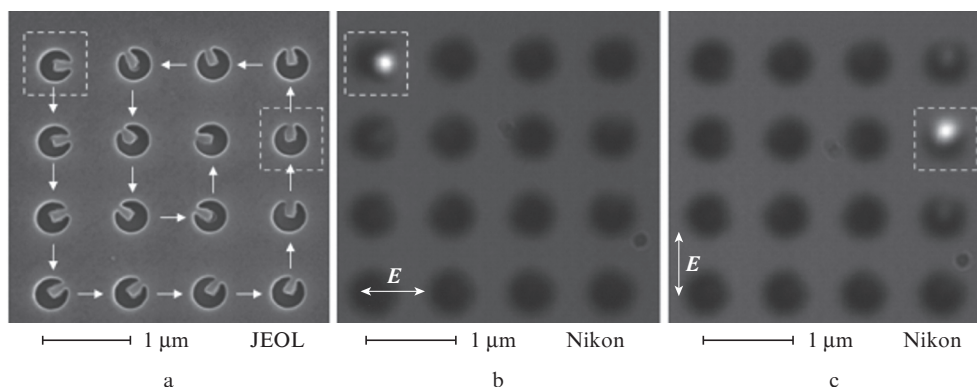


**Figure 5.** Completely optical display based on SHR NS's [23]: (a) electron-microscope image of optical display: SHR nanostructures are formed in a 100-nm-thick aluminium film in the form of a  $4 \times 4$  array with a step of  $1 \mu\text{m}$  (the sequence of nanostructure fabrication is indicated by arrows; the rod of each subsequent nanostructure is rotated by an angle of about  $11.5^\circ$  with respect to the previous one); (b) optical-microscope image of the display exposed to light with a polarisation vector directed along the nanorod of the first SHR NS (is framed); and (c) optical-microscope image of the display exposed to light with a polarisation vector directed along the nanorod of the last SHR NS (is framed). The arrows in Figs 5b and 5c show the directions of the polarisation vectors of excitation light.

Nanostructures are formed in a 100-nm-thick aluminium film. The nanorod of each SHR NS is rotated with respect to the nanorod of a neighbouring (next) nanostructure by an angle of  $11.5^\circ$  (Fig. 5a). The principle of operation of this display is as follows. All SHR NS's are irradiated by a femtosecond laser beam with  $\lambda = 1560 \text{ nm}$ . For the incident light linearly polarised along the nanorod of one of the SHR NS's, only this nanostructure is in exact resonance with field at the fundamental frequency of femtosecond radiation, and this nanostructure becomes an efficient third-harmonic radiation source. Thus, having chosen a certain polarisation vector of radiation, one can 'switch on' particular display pixels.

The measurement results, which demonstrate the principle of operation of an all-optical display, are shown in Figs 5b and 5c. When the polarisation vector of femtosecond radiation is rotated, it is tuned in resonance with one of the display SHR NS's, and the latter becomes a third-harmonic radiation source. For example, when the upper left pixel of the display in Fig. 5a is addressed to (this SHR NS is framed), the polarisation vector is chosen to be directed along the nanorod. In this case, display illumination causes luminescence of only this pixel (at the third-harmonic frequency) (Fig. 5b). When the polarisation vector is rotated by  $90^\circ$ , its direction coincides with that of nanorod in another SHR (in Fig. 5a, this nanostructure in the right column is framed), which is brought into resonance with the incident light and luminescence from only this pixel occurs (Fig. 5c).

We experimentally observed the display operation using an additional halogen lamp, which illuminated the display and made it possible to identify unambiguously the spatial position of a luminous pixel. A bandpass filter (10-nm wide) was used to cut out a wavelength of 520 nm from the lamp emission spectrum; this radiation was directed to the sample through the same objective ( $\text{NA} = 1.49$ ) that was used to collect the third-harmonic radiation. The illumination at a frequency near the THG frequency made it possible to eliminate the influence of the objective chromatic aberration. Due to the illumination, one can see (in scattered light) all SHR NS's forming the optical display in the form of dark spots against the scattering background from the aluminium film (Figs 5b, 5c).

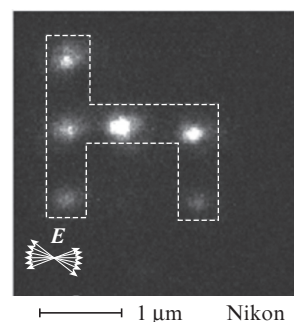


**Figure 6.** A simple image in the form of a letter h obtained with an all-optical display [23] excited by radiation at 1560 nm (polarisations are shown by arrows). The dashed line shows SHR NS's which are in resonance with excited radiation.

Figure 6 presents implementation of a very simple image in the form of letter h using the above-described display. In our experiment the polarisation of excitation light was rotated at certain angles to bring femtosecond radiation into resonance with 'necessary' SHR NS's of the display (shown by dotted line in Fig. 6). It can be seen that the image obtained at the third-harmonic frequency consists of diffraction-limited spots forming a letter h.

To increase the spatial resolution of the display, we tried to reduce the distance between SHR NS's. It is well known that resonant plasmon nanostructures are sensitive to the optical properties of their environment. When identical nanostructures are located closely, their resonance frequency is shifted with respect to that of individual nanostructures. We used samples with SHR arrays with different distances between nanostructure centres. The measurements showed that even closely located SHR NS's (spaced by 500 nm, which is about  $1/3$  excitation wavelength) allow for independent control of THG by changing the polarisation of light. The contrast was measured to be about 5. Note also a possibility of ultrafast control of pixels of the optical display presented here: the characteristic relaxation times of plasmon oscillations in aluminium may be as short as approximately 100 as [24].

## 4. Conclusions

We investigated the nonlinear properties of single plasmonic nanostructures. The new element of nano-optics and nano-photonics – SHR – was found to be a very interesting object. It is characterised by the following unique properties: (i) provides a record-high THG efficiency from a single nanostructure, which exceeds the corresponding efficiency of a nanohole by five orders of magnitude, and an unprecedentedly high efficiency of multiphoton luminescence; (ii) has pronounced polarisation properties; (iii) can be used to design a nanolocalised light source with a spatial localisation of about  $\lambda/15$ ; and (iv) allows for an all-optical control of nanolocalised light sources located at distances to  $\lambda/3$ . Note also that the SHR NS efficiency can be increased even more using photonic-crystal microcavities [25–28].

**Acknowledgements.** This work was supported in part by the Russian Foundation for Basic Research (Grant Nos 11-02-00804-a, 12-02-00784-a, and 13-02-01281), the Russian Research Foundation and the Presidium of the Russian Academy of Sciences (Extreme Light Fields and Their Applications Programme).

## References

1. Boyd R.W. *Nonlinear Optics* (London: Acad. Press, 2003) p. 127.
2. Palomba S., Danckwerts M., Novotny L. *J. Opt. A*, **11**, 114030 (2009).
3. Bouhelier A., Beversluis M., Hartschuh A., Novotny L. *Phys. Rev. Lett.*, **90**, 013903 (2003).
4. Labardi M. et al. *Opt. Lett.*, **29**, 62 (2004).
5. Stockman M.I. et al. *Phys. Rev. Lett.*, **92**, 057402 (2004).
6. Zheludev N.I., Emelyanov V.I. *J. Opt. A*, **6**, 26 (2004).
7. Canfield B.K. et al. *Nano Lett.*, **7**, 1251 (2007).
8. Renger J., Quidant R., van Hulst N., Novotny L. *Phys. Rev. Lett.*, **104**, 046803 (2010).
9. Kim S. et al. *Nature*, **453**, 757 (2008).
10. Park I.Y. et al. *Nature Photon.*, **5**, 677 (2011).
11. Utikal T. et al. *Phys. Rev. Lett.*, **104**, 113903 (2010).
12. Pacifici D., Lezec H.J., Atwater H.A. *Nature Photon.*, **1**, 402 (2007).
13. MacDonald K.F., Samson Z.L., Stockman M.I., Zheludev N.I. *Nature Photon.*, **3**, 55 (2009).
14. Liu Z.Y. et al. *Laser Phys. Lett.*, **9**, 649 (2012).
15. Imura K., Nagahara T., Okamoto H. *J. Phys. Chem. B*, **109**, 13214 (2005).
16. Farrer R.A., Buttereld F.L., Chen V.W., Fourkas J.T. *Nano Lett.*, **5**, 1139 (2005).
17. Biagioni P. et al. *Phys. Rev. B*, **80**, 045411 (2009).
18. Biagioni P. et al. *Nano Lett.*, **12**, 2941 (2012).
19. Shahbazyan T.V. *Nano Lett.*, **13**, 194 (2003).
20. Melentiev P.N. et al. *Opt. Express*, **21**, 13896 (2013).
21. Melentiev P.N. et al. *Laser Phys. Lett.*, **10**, 075901 (2013).
22. Konstantinova T.V. et al. *Zh. Eksp. Teor. Fiz.*, **144**, 27 (2013).
23. Melentiev P.N. et al. *Opt. Lett.*, **38**, 2274 (2013).
24. Stockman M.I., Kling M.F., Kleineberg U., Krausz F. *Nature Photon.*, **1**, 539 (2007).
25. Melentiev P.N. et al. *Opt. Express*, **19**, 22743 (2011).
26. Melentiev P.N. et al. *Opt. Express*, **20**, 19474 (2012).
27. Melentiev P.N., Afanasiev A.E., Balykin V.I. *Phys. Rev. A*, **88**, 053841 (2013).
28. Treshin I.V., Klimov V.V., Melentiev P.N., Balykin V.I. *Phys. Rev. A*, **88**, 023832 (2013).